solution of 1,3-cyclohexadiene in CH_2Cl_2 at 0 °C. The product was purified by gas chromatography on Column a; IR 3050, 2950, 2900, 1465, 1440, 1380, 1315, 1280, 1215, 1155, 1085, 1055, 1040, 950, 925, and 858 cm^{-1}. The NMR spectrum agreed with the published one.[25]

Pentane (Baker-Photrex grade) was uniformly used as the solvent for photolysis.

Apparatus. The equipment for photolyses at 185 nm in solution either on a preparative scale (0.1–0.5 g) or for kinetic studies has been described.[26] An Acton 185 band-pass filter was used to isolate the 185-nm line in quantitative studies. Ultraviolet absorption spectra were recorded on a Cary 17D spectrometer. The digitized output could be stored in a computer. Solutions of two compounds (e.g., **3** and **4**) at an identical concentration were separately scanned in the spectrometer by using the same cell to obtain the difference spectrum between the compounds. The spectra were stored, then subtracted, and displayed. The difference spectra could be amplified suitably to emphasize minor dissimilarities.

Procedure. A solution of the tricyclic ene ($\sim 5 \times 10^{-3}$ M) in pentane was placed in a cylindrical cell (volume, 9.3 mL) with a Suprasil window and flushed with nitrogen. Photolyses were carried to conversions of <20%. Aliquots were withdrawn at various time intervals and analyzed on a Perkin-Elmer 3920B gas chromatograph fitted with a Carbowax column (14 ft × $^1/_8$ in.) and both thermal conductivity and flame ionization detectors. In the case of **2**, a gum rubber column was used in addition to separate **2** from **1**. The detectors were calibrated from time to time with bicyclo[2.2.2]octane as reference.

Photolysis of 1. Irradiation was carried out as described above. Separation by gas chromatography (Columns a and c) showed the presence of diene **8** (14%) and tetracyclic hydrocarbon **10** (36%). Diene **8** was prepared by the method of Moore, Moser, and LaPrade.[27] The NMR spectrum [δ 6.07 (1 H, q), 5.86 (1 H, q), 5.53 (1 H, br d), 5.03 (1 H, complex), 1.5–2.7 (6 H)] agreed with the published[27] one. Product **10** agreed in its IR and NMR spectra [δ 1.8 (5 H), 1.4 (5 H)] with the published[27] spectra.

Photolysis of 2. Following irradiation as described above, separation was carried out by gas chromatography on Columns a and b. The three major products were **8** (28%), **9** (23%), and **10** (26%). Product **9** [NMR δ 5.9 (2 H), 2.6 (1 H), 1.6 (5 H), 1.2 (1 H), 0.9 (1 H), and 0.7 (1 H)] fully agreed in its NMR spectrum with the spectra in the literature.[8]

Photolysis of 3. There was a single product, **13**, formed in 55% yield. Remaining products amounted to <5%. Separation was carried out by gas chromatography on Columns a and b.

Tetracyclo[4.3.0.0^{2,9}0^{5,7}]nonane (13): M_r (mass spectrum) 120 (base peak 79); IR 3008 (s), 3001 (s), 2900 (s), 1470, 1460, 1440, 1340, 1050, 940, 850, 690 cm^{-1}; NMR δ 0.4–0.9 (10 H, m), 0.9–2.1 (2 H, m).

Photolysis of 4. There were two main products which were separated by gas chromatography on Columns a and b. These were **12** (22%) and **13** (5%). The spectra of **12** agreed with those of an authentic sample kindly furnished by Professor G. W. Klumpp.

Photolysis of Diene 8 at 185 nm. A solution of **8** in pentane (3×10^{-3} M) was photolyzed with the isolated 185-nm radiation. The products that were observed (in decreasing importance) were **11**, **9**, and an unknown. The ratio of **9** to **11** was $\sim$1:3, which is of the same order as was reported by Sauers and Shurpik[8] in direct photolysis at longer wavelengths. Note that the ratio of **9** to **11** is reversed in importance when triplet sensitization *in solution* is used.[8]

Acknowledgments. We thank Mr. Robert Fern of the Research Center for the ultraviolet spectra and Dr. G. W. Klumpp of the Free University of Amsterdam for the NMR spectrum of **10**.

---

(25) G. R. Wenzinger and J. A. Ors, *J. Org. Chem.*, **39**, 2060 (1974).

(26) R. Srinivasan and L. S. White, *J. Am. Chem. Soc.*, **101**, 6389 (1979).

(27) W. R. Moore, W. R. Moser, and J. E. LaPrade, *J. Org. Chem.*, **28**, 2205 (1963).

Potential Surfaces for $(NH)_3^{2+}$

Weston Thatcher Borden,* Ernest R. Davidson, and David Feller

Contribution from the Department of Chemistry, University of Washington, Seattle, Washington 98195. *Received January 28, 1980*

Abstract: Potential surfaces for the lowest triplet and two lowest singlet states of the triaziridenyl dication, a molecule isoelectronic with the cyclopropenyl carbanion, have been obtained from ab initio calculations. It is found that when the σ core is allowed to deviate from D_{3h} symmetry, the two lowest singlet states, at the SCF or π CI level of theory, are nondegenerate by 13 kcal/mol at D_{3h} geometries. The lower state, $^1A_1$, also fails to exhibit even qualitatively correct behavior on molecular distortion to geometries of C_{2v} symmetry. It is shown by group-theoretical arguments that CI in the σ space must accompany π CI in order to obtain satisfactory $^1E'$ wave functions. σ–π CI calculations are, in fact, found to yield singlet wave functions that exhibit both D_{3h} degeneracy and the correct Jahn–Teller behavior on molecular distortions to C_{2v} symmetry. A modified CI protocol has been developed to explore nonplanar molecular geometries. It is found that all three of the lowest states of $(NH)_3^{2+}$ prefer such geometries; the stationary points on the global surfaces for these states have been obtained. A substantial barrier to pseudorotation is predicted for the lowest singlet, which is calculated to be the ground state of the molecule. The driving force for nitrogen pyramidalization in $(NH)_3^{2+}$ is discussed in light of population analyses at planar and nonplanar geometries.

Several years ago, as part of a continuing series of studies of the potential surfaces for molecules containing open-shell π systems, we carried out calculations on the planar cyclopropenyl anion.[1] The aim of this project was to verify computationally a prediction of the location of the minima on the potential surface for the lowest singlet state, based on consideration of first- and second-order Jahn–Teller effects. Despite the fact that the computed surface was found to have the form expected, several aspects of our calculations were somewhat unsatisfactory, as we ourselves noted.[1]

First, the energy of the $^3A_2'$ ground state of the planar anion was found to be 6.7 eV above that of the lowest doublet state of the planar cyclopropenyl radical, for which we also carried out calculations.[1] Therefore, if increasingly diffuse basis functions had been added to the minimal STO-3G set used, the energy of the anion would have been greatly reduced, until, if a complete basis set were used in the π space, the extra electron in the planar anion would almost certainly not have been found to be bound.[2]

---

(1) Davidson, E. R.; Borden, W. T. *J. Chem. Phys.* **1977**, *67*, 2191.

(2) It would, in fact, be rather surprising if the planar cyclopropenyl anion were bound in the gas phase, since the pyramidal methyl anion is found experimentally to be bound by less than 2 kcal/mol[3] and Breslow's study of a presumably nonplanar cyclopropenyl anion in solution shows that even this species is conjugatively destabilized.[4,5]

(3) Ellison, G. B.; Engelking, P. C.; Lineberger, W. C. *J. Am. Chem. Soc.* **1978**, *100*, 2556.

(4) Breslow, R.; Goodin, R. *J. Am. Chem. Soc.* **1976**, *98*, 6076. Wasielewski, M. R.; Breslow, R., *Ibid.* **1976**, *98*, 4222.

0002-7863/80/1502-5302$01.00/0

Thus, as we pointed out, our STO-3G results probably have little relevance to the cyclopropenyl anion in the gas phase, although they might give some indication of what could be expected for this species in solution.

Whether our results actually do have any relevance to the behavior of the cyclopropenyl anion in solution is also open to question, since our calculations were restricted to the planar molecule. We noted that pyramidalization would stabilize the geometry of the singlet that corresponds to a wave function which places a strong π bond between two carbons and a localized pair of π electrons at the third (**1**). Indeed, Clark has found that at the C–C bond lengths of cyclopropene, pyramidalization lowers the calculated energy of the lowest singlet state of the anion by 52.3 kcal/mol at the SCF level.[6] By analogy with the results obtained by Poppinger and Radom for the cyclopropenyl radical,[7] there are also other geometries (e.g., **2**) at which pyramidalization might be expected to effect stabilization of the lowest singlet state of the anion.

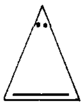

1

2

These two criticisms of our calculations, dealing with their chemical relevance, are certainly valid. However, as mentioned above, the goal of our study was not the accurate description of the cyclopropenyl anion in the gas phase but rather a computational verification of the predicted shape of the potential surface for the lowest singlet state of a planar molecule containing a cyclic, four-electron, three-orbital π system. A much more serious criticism of our calculations concerns the methodology used to carry them out.

With the imposition of D_{3h} symmetry, the π-electron wave functions for two components of the degenerate $^1E'$ state of the cyclopropenyl anion at the SCF level are

$$^1E_x' = |a_2''^2 e_x'' e_y''(\alpha\beta - \beta\alpha)\rangle \tag{1}$$

$$^1E_y' = |a_2''^2 e_x''^2\rangle - |a_2'' e_y''^2\rangle \tag{2}$$

Thus, a two-configuration SCF wave function is required to properly describe $^1E_y'$ at D_{3h} geometries. Since we did not have an MCSCF routine available at the time we carried out our previous study, we used the orbitals obtained from SCF calculations on the triplet state to generate singlet configurations for full CI in the π space. If the σ cores of $^3A_2'$ and $^1E'$ were identical, the $^3A_2'$ and $^1E'$ π MO's would have led to the same $^1E'$ CI wave function.[8] However, recent calculations on the isoelectronic cyclopentadienyl cation have shown that in this molecule the σ cores of $^3A_2'$ and of the two components of $^1E'$ are sufficiently different at the SCF level that the π-space CI energy of the lowest singlet states depends on which set of MO's is used.[9] Moreover, it was found that in the cation the MO's of the triplet became progressively worse for the CI description of the singlet states as the molecule distorted away from D_{5h} symmetry. Thus, it appeared possible that our singlet surface for the planar cyclopropenyl anion, based as it was on CI energies obtained with MO's from triplet SCF calculations, might be in error.

An obvious check on our previous cyclopropenyl anion results was to repeat the π-space CI calculations, using the MO's from SCF or MCSCF calculations on the appropriate singlet state to carry out CI calculations for that state. As has been pointed out previously,[8,10] it is essential, in order to obtain optimal SCF wave functions for an $^1E'$ state, to impose only C_{2v} symmetry on the MO's. Thus, the SCF π wave functions for the two lowest singlet states of the cyclopropenyl anion must, even at D_{3h} geometries, be described as belonging only to representations of this subgroup of D_{3h}. The two lowest singlet SCF wave functions are, therefore

$$^1B_2 = |1b_1^2 a_2 2b_1(\alpha\beta - \beta\alpha)\rangle \tag{3}$$

$$^1A_1 = c_1|1b_1^2 a_2^2\rangle - c_2|1b_1^2 2b_1^2\rangle \tag{4}$$

When the $^1B_2$ RHF and $^1A_1$ MCSCF orbitals were generated and used for π-space CI calculations, it was found that lower CI energies were, in fact, obtained than when the orbitals from the $^3B_2$ SCF calculation were employed.[11] However, even at a D_{3h} molecular geometry, the energies of the $^1B_2$ and $^1A_1$ CI wave functions were not identical, as they would have been for pure $^1E'$ wave functions. In fact, at a C–C bond length of 1.44 Å the two singlets were found to be nondegenerate in energy by more than 6 kcal/mol. Since the relative energies of the two wave functions at distorted geometries determine the nature of the lowest singlet potential surface for cyclopropenyl anion, it is obvious that wave functions that differ by more than 6 kcal/mol at a point at which they should be degenerate cannot provide useful information about the surface.[12]

The present study was initiated in an effort to carry out satisfactory calculations for the lowest singlet potential surface of a planar molecule containing a cyclic, three-orbital, four-electron π system. Rather than reexamining the cyclopropenyl anion, we chose the isoelectronic $(NH)_3^{2+}$ for study.[13] The additional charge on each heavy-atom nucleus of $(NH)_3^{2+}$ should guarantee that, unlike the case in the cyclopropenyl anion, all the electrons in this dication would be bound in the gas phase, thus rendering ab initio calculations relevant to the unsolvated species. We have carried out calculations at both planar and nonplanar geometries, in order to provide a more global and, hence, more chemically useful description of $(NH)_3^{2+}$.

Theoretical Considerations

The cause of the lack of D_{3h} degeneracy of the $^1B_2$ and $^1A^1$ π CI wave functions, based, respectively, on $^1B_2$ SCF and $^1A_1$ MCSCF MO's, is distortion of the σ cores from D_{3h} symmetry. Each component of a pure $^1E'$ π wave function gives a charge distribution that by itself has only C_{2v}, not D_{3h}, symmetry.[1] In the presence of a C_{2v} π-charge distribution the σ core can be expected also to deviate from D_{3h} symmetry if it is allowed to do so. In contrast, even when only C_{2v} symmetry is imposed on the MO's, the σ core from SCF calculations on the lowest triplet maintains D_{3h} symmetry at D_{3h} geometries because the π-charge distribution for an $^3A_2'$ state has the full molecular symmetry.[15] This explains why the σ core from the SCF calculation on each singlet state of cyclopropenyl anion gives a lower π CI energy for that state than does the σ core from the triplet SCF calculation, since the D_{3h} σ core of the triplet is not optimal for the π CI wave function of either singlet.

Since the σ cores of the singlets are obtained at the SCF level, it might be imagined that they are also less than optimal for the π-space CI wave functions. Were this true, reoptimization of the σ MO's not only would lower the energy of the singlet π CI wave functions but also might restore their degeneracy at D_{3h} geometries. However, the σ core of $^1B_2$ is, in fact, optimal for the π CI wave function. This follows from the fact that, because of the small

---

(5) Breslow, R. *Acc. Chem. Res.* **1973**, *6*, 393.

(6) Clark, D. T. *Chem. Commun.* **1969**, 637.

(7) Poppinger, D.; Radom, L.; Vincent, M. A. *Chem. Phys.* **1977**, *23*, 437.

(8) See, for instance: Borden, W. T. *J. Am. Chem. Soc.* **1976**, *98*, 2695; Davidson, E. R.; Borden, W. T. *J. Chem. Phys.* **1976**, *64*, 663.

(9) Borden, W. T.; Davidson, E. R. *J. Am. Chem. Soc.* **1979**, *101*, 3771.

(10) Manne, R. *Mol. Phys.* **1972**, *24*, 935.

(11) Tanaka, K.; Davidson, E. R.; Borden, W. T., unpublished results.

(12) The same problem was encountered in calculations on the cyclopentadienyl cation.[9] However, in the cation the first- and second-order Jahn–Teller effects occur along different distortion coordinates, so the relative energies of $^1B_2$ and $^1A_1$ are of much less importance in determining the nature of the potential surface for the lowest singlet state.

(13) Although $(NH)_3^{2+}$ is as yet apparently unknown, it might, for instance, be prepared by two-electron oxidation of triaziridine.[14]

(14) Yang, K.; Gilje, J. W.; Seff, K. *J. Am. Chem. Soc.* **1977**, *99*, 7057.

(15) The electric field association with a $^3A_2'$ wave function belongs to the $[A'_2]^2 = A_1'$ representation of D_{3h}. In contrast, the field associated with $^1E_x'$ or $^1E_y'$ belongs to $A_1' + E_y'$ and is thus invariant only under the C_{2v} subgroup of D_{3h}, wherein both A_1' and E_y' of D_{3h} correspond to A_1.

number of configurations that can be generated within a minimal basis set when four electrons occupy three MO's, the $^1B_2$ SCF and π CI wave functions are identical. In contrast, the fact that the $^1A_1$ MCSCF π wave function can be improved by CI suggests that, after CI, the σ core really may not be optimal for the π wave function of this state. Nevertheless, despite the fact that the σ core of the former singlet state is optimal for its π CI wave function while that of the latter is probably not, $^1B_2$ lies above $^1A_1$. It thus becomes obvious that degeneracy between $^1B_2$ and $^1A_1$ cannot be restored by reoptimizing the σ cores by an SCF procedure. One is forced to conclude that in calculations where the σ core is distorted by a nontotally symmetric distribution of π charge, pure $^1E'$ wave functions can only be obtained by carrying out CI in both the π and σ spaces. This conclusion is reached because there is no other reasonable possibility for improving the $^1B_2$ wave function, relative to the $^1A_1$, for the cyclopropenyl anion. The same conclusion is arrived at more directly by a group-theoretical analysis of what must be done to obtain a pure $^1E_x'$ wave function from one constrained to belong to only the $^1B_2$ representation of the C_{2v} subgroup of D_{3h}.

It is easy to verify that the only two $^1B_2$ π configurations, written in terms of D_{3h} MO's, are $|a_2''^2 e_x'' e_y''(\alpha\beta - \beta\alpha)\rangle$ and $|a_2'' e_x'' e_y''^2(\alpha\beta - \beta\alpha)\rangle$. Both of these are pure $^1E_x'$ in D_{3h}; therefore, the $^1B_2$ π CI wave function must also belong to this irreducible representation of D_{3h}. As noted above, even a pure $^1E_x'$ wave function, in general, gives rise to a distribution of π charge with only C_{2v} symmetry, resulting in a corresponding distortion of the electron density in the σ core. This distortion arises from mixing of a_1' with e_y', both of which are a_1 in C_{2v}, and of a_2' with e_x', both of which belong to b_2 in C_{2v}. These two types of excitations are both of E_y' symmetry in the full D_{3h} point group. Therefore, the $^1B_2$ wave function, written in terms of D_{3h} representations, may be expressed as

$$^1B_2 = {}^1E_x'(\pi)[{}^1A_1'(\sigma) + \sum_i \lambda_i {}^1E_y'(\sigma)_i + ...] \quad (5)$$

The first term in brackets represents the undistorted σ core that could be obtained from, for instance, a calculation on the $^3A_2'$ state, while the summation is over those one-electron excitations of E_y' symmetry that distort the σ core. There are also terms in the sum that represent products of one-electron excitations. These terms, not written out explicitly in eq 5, are present in the $^1B_2$ σ wave function determined at the SCF level. Like the terms that have been written out in eq 5, the product terms span the $^1A_1'$ and $^1E_y'$ representations of D_{3h}. If the λ_i are small, the product terms should be less important than the terms that are linear in the λ_i; therefore, for the present, the nonlinear terms will be ignored.

An $^1E_x'$ π wave function coupled to an $^1A_1'$ σ wave function belongs, of course, to the $^1E_x'$ representation of D_{3h}. However, an $^1E_x'$ π wave function coupled to one of $^1E_y'$ symmetry in the σ space is a mixture of $^1E_x'$ and $^1A_2'$ symmetries. This is most easily demonstrated by writing out pure $^1E_x'$ and $^1A_2'$ product wave functions of this type and seeing that their sum has the form of the terms in the summation in eq 5.

$$^1E_x' = {}^1E_x'(\pi){}^1E_y'(\sigma) + {}^1E_y'(\pi){}^1E_x'(\sigma) \quad (6)$$

$$^1A_2' = {}^1E_x'(\pi){}^1E_y'(\sigma) - {}^1E_y'(\pi){}^1E_x'(\sigma) \quad (7)$$

Equation 6 provides the answer to the question of how to obtain a pure $^1E_x'$ wave function when a π wave function of this symmetry results in distortion of the σ core. In order to transform the terms in the summation in eq 5 into ones of pure $^1E_x'$ symmetry, each σ excitation of $^1E_y'$ symmetry that is coupled to an $^1E_x'$ π wave function must be accompanied by an $^1E_x'$ excitation from the optimum $^1A_1'$ σ core that is coupled to a π wave function of $^1E_y'$ symmetry. This must be done not only for the one-electron excitations that are linear in λ_i but also for the multiple excitations that involve products of the λ_i. Thus, transforming a $^1B_2$ SCF wave function, obtained with only C_{2v} symmetry imposed on the MO's, into one of pure $^1E_x'$ symmetry requires a very extensive CI in which the $^1B_2(\pi)^1A_1(\sigma)$ SCF wave function is allowed to mix with excited configurations of the form $^1A_1(\pi)^1B_2(\sigma)$. Excitations in the σ space of the same order as the highest order product of the λ_i in eq 5 have to be included in order to guarantee a wave function of pure $^1E_x'$ symmetry. Nevertheless, the terms that are linear in the λ_i, which involve just single excitations, should be the most important.

An alternative, which requires only single excitations in the σ space, is to start with D_{3h}-symmetry MO's, obtained, for instance, from an SCF calculation on $^3A_2'$. The σ core can be allowed to distort in the presence of the $^1E_x'$ π wave function by permitting one-electron excitations of $^1E_y'$ symmetry in the σ space. However, these excitations, in order to preserve the overall $^1E_x'$ symmetry of the wave function, have to be accompanied by simultaneous $^1E_x'$ excitations in both the π and σ spaces, which yield terms of the second type in eq 6. Thus, a pure $^1E_x'$ wave function that allows for distortion of the σ core takes the form

$$^1E_x' = {}^1E_x'(\pi){}^1A_1'(\sigma) + \sum_i \lambda_i[{}^1E_x'(\pi){}^1E_y'(\sigma)_i + {}^1E_y'(\pi){}^1E_x'(\sigma)_i] \quad (8)$$

The corresponding $^1E_y'$ wave function is

$$^1E_y' = {}^1E_y'(\pi){}^1A_1'(\sigma) + \sum_i \lambda_i[{}^1E_y'(\pi){}^1E_y'(\sigma)_i - {}^1E_x'(\pi){}^1E_x'(\sigma)_i] \quad (9)$$

In both equations the last set of terms provide σ–π correlation in the x direction. Symmetry dictates that in order to have a pure $^1E'$ wave function, σ–π correlation parallel to the x axis must accompany the distortion of the σ MO's that occurs along the y axis. From the point of view of symmetry, these two superficially different consequences of the Coulombic repulsion between σ and π electrons are seen to be closely linked.

Calculations at D_{3h} Geometries. Calculations on $(NH)_3^{2+}$ were carried out with an STO-3G basis set.[16] Previous experience with π CI calculations on trimethylenemethane[17] and cyclobutadiene[18] has shown that, at least with these systems, the STO-3G basis gives relative energies that are comparable to those obtained with higher quality basis sets.

RHF calculations on the lowest triplet state were carried out in order to obtain MO's from which pure $^1E'$ wave functions could be generated. Because only C_{2v} symmetry was imposed on the MO's, the AO coefficients deviated slightly in the third significant figure from those required for pure D_{3h} orbitals, despite the fact that the SCF energy was converged to 10^{-7} hartree. The MO's from these $^3B_2$ SCF calculations were used to carry out CI on the two lowest singlet states, $^1B_2$ and $^1A_1$, in C_{2v} symmetry. The three lowest energy MO's, corresponding to the three nitrogen 1s orbitals, were frozen, and single excitations from the remaining six filled σ orbitals into all six virtual σ orbitals were allowed for *all* π configurations. This σ–π CI procedure generated 164 $^1B_2$ and 166 $^1A_1$ space–spin product configurations and guaranteed that among these would be the pairs of configurations required by eq 8 and 9. The CI energies of the two singlet states were the same to better than 10^{-4} hartree, and the atomic and overlap populations showed the relationships expected for $^1E_x'$ and $^1E_y'$ wave functions.[1,9,19] Thus, as anticipated, this type of σ–π CI, using MO's of close to pure D_{3h}-symmetry, did succeed in producing the two components of a $^1E'$ state.

The same type of CI calculations on the lowest triplet state of $(NH)_3^{2+}$ were also carried out with RHF $^3B_2$ MO's. The CI

---

(16) Hehre, W. J.; Stewart, R. F.; Pople, J. A. *J. Chem. Phys.* **1969**, *51*, 2657.

(17) Davidson, E. R.; Borden, W. T. *J. Am. Chem. Soc.* **1977**, *99*, 2053.

(18) Borden, W. T.; Davidson, E. R.; Hart, P. *J. Am. Chem. Soc.* **1978**, *100*, 388.

(19) The π overlap populations by themselves did not exhibit the relationships expected for $^1E_x'$ and $^1E_y'$ π wave functions. This is not surprising, since only the total wave functions, and not the π and σ components individually, belong to pure representations of D_{3h}. Also as expected, when the terms of the third type in eq 8 and 9 were omitted from the CI, distinctly nondegenerate total wave functions were obtained. When $^3A_2'$ MO's were used, the energies of the two wave functions differed by more than 0.03 hartree (almost 20 kcal/mol).

Table I. State Energies of $(NH)_3^{2+}$ at a D_{3h} Geometry[a]

state	type of wave function	energy, hartrees
$^1B_2$	RHF	−161.8990
$^1A_1$	MCSCF	−161.9200
$^1B_2$	π CI	−161.8990
$^1A_1$	π CI	−161.9204
$^1B_2$	σ–π CI[b] with $^1B_2$ MO's	−161.9942
$^1A_1$	σ–π CI[b] with $^1A_1$ MO's	−161.9903
$^1B_2$ ($^1E_x'$)	σ–π CI[b] with $^3B_2$ MO's	−161.9959
$^1A_1$ ($^1E_y'$)	σ–π CI[b] with $^3B_2$ MO's	−161.9959
$^3B_2$ ($^3A_2'$)	σ–π CI[b] with $^3B_2$ MO's	−162.0415[c]

[a] $r_{N-N} = 1.432$ Å, $r_{N-H} = 1.106$ Å. This is the optimal D_{3h} geometry for the $^1E'$ σ–π CI wave function.[b] [b] The CI included all single σ valence excitations for all possible π configurations. [c] At the optimal $^3A_2'$ geometry with $r_{N-N} = 1.416$ Å the energy is −162.0422 hartree.

energies were used to optimize the N–H and N–N bond lengths. The values obtained were, respectively, 1.106 and 1.416 Å. Population analyses showed the atomic and overlap populations to possess D_{3h} symmetry, so that the lowest triplet state is truly $^3A_2'$, even though only C_{2v} symmetry was imposed on the wave function.

The optimal D_{3h} geometry for the $^1E'$ CI wave function was found to have $r_{N-H} = 1.106$ Å and $r_{N-N} = 1.432$ Å. The longer N–N bonds in this state, compared to those in $^3A_2'$, are due to the fact that electron repulsion in this singlet state causes the D_{3h} orbitals of $^3A_2'$ to be nonoptimal for $^1E'$. Since the $^3A_2'$ MO's provide maximum N–N overlap populations, the average N–N overlap population in $^1E'$ is smaller than that in $^3A_2'$—hence the longer bonds in the singlet state.

At the optimal $^1E'$ geometry, $^1B_2$ RHF and $^1A_1$ two-configuration MCSCF wave functions were computed. The MO's were used to carry out $^1B_2$ and $^1A_1$ CI calculations, again allowing all single excitations from filled to unfilled σ valence orbitals for all π configurations. Population analyses showed that the atomic and overlap populations for the CI wave functions, based on the $^1B_2$ and $^1A_1$ SCF calculations, did not exhibit the complementary relationships expected for $^1E_x'$ and $^1E_y'$ wave functions. The energies of the two lowest singlet states were not found to be degenerate either. As shown in Table I, not only did the energies differ by 2.5 kcal/mol but both were above that of the degenerate pair of singlet wave functions, obtained using the nearly pure D_{3h}-symmetry orbitals of the triplet.

The lower energy calculated for the CI wave function based on D_{3h}-symmetry MO's is presumably due to the fact that it is of pure $^1E'$ symmetry. Hence, it is uncontaminated by the excited $^1A_2'$ and $^1A_1'$ D_{3h} symmetry states that pollute, respectively, the $^1E_x'$ and $^1E_y'$ wave functions when the MO's from the singlet SCF calculations are used for the CI. The presence of these contaminants in the $^1B_2$ and $^1A_1$ wave functions raises their energies above that of the pure $^1E'$ wave functions that are obtained with the MO's from the triplet SCF calculation.

It should be noted that although the σ–π CI wave functions based on the singlet SCF MO's are not of pure $^1E'$ symmetry, they are much closer to being degenerate than the $^1B_2$ and $^1A_1$ SCF wave functions. As shown in Table I, the SCF wave functions differ in energy by 13.1 kcal/mol, more than 5 times larger an amount of energy than when σ–π CI is included. Carrying out π CI alone merely serves to increase the lack of degeneracy, albeit by merely 0.0004 hartree, since, as noted above, only $^1A_1$ profits from π CI with a minimal basis set. σ–π CI reduces the energy difference between $^1B_2$ and $^1A_1$ (and incidentally changes its sign) by annihilating the $^1A_2'$ and $^1A_1'$ contaminants that are linear in the λ_i, thus yielding wave functions that are more nearly of pure $^1E_x'$ and $^1E_y'$ symmetry.

Presumably, further CI, involving higher excitations in the σ valence orbital space, would yield even more nearly degenerate singlet wave functions. However, inclusion of just double excitations in the σ space for all π configurations would add 1874 $^1B_2$ and 2670 $^1A_1$ new orbital occupancies to the configuration lists. Since for some of these there can be several different singlet spin couplings, the CI would grow very large indeed, even for a minimal basis set calculation. Therefore, the preferred technique for obtaining pure $^1E'$ wave functions, at least with a minimal basis set, is to use the MO's from the $^3B_2$ RHF calculation, rather than those from the $^1B_2$ RHF or $^1A_1$ MCSCF, to carry out σ–π CI.

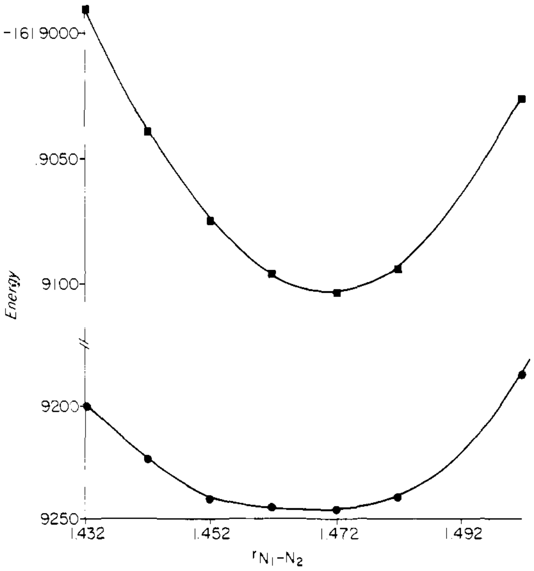

Figure 1. Energies of two-configuration MCSCF $^1A_1$ (●) and RHF $^1B_2$ (■) wave functions on negative e_y' distortions from $r_{N-N} = 1.432$ Å. For such distortions $r_{N_1-N_2} = r_{N_1-N_3} = 2.148 - {}^1/_2 r_{N_2-N_3}$.

Calculations at C_{2v} Geometries. The Jahn–Teller theorem predicts that a molecule in an $^1E'$ state can lower its energy by distorting away from D_{3h} symmetry in a mode of e′ symmetry.[20] In addition to the first-order Jahn–Teller effect, there is a second-order effect[21] that comes from the mixing of $^1E'$ with $^1A_1'$ on molecular distortion away from D_{3h} symmetry. The latter state has the same form as $^1E_y'$ at the SCF level, except for a change in the sign between the two configurations in eq 2. Therefore, $^1A_1'$ is relatively low in energy, so that its mixing with the lowest singlet state on molecular distortion has important consequences in antiaromatic annulenes[1,9,18] and also in trimethylenemethane.[17] We have previously shown that in planar cyclopropenyl anion the interplay of first- and second-order effects produces a minimum on the potential surface for pseudorotation along the positive e_y' distortion coordinate and a saddle point along negative e_y'.[1] An e_y' distortion preserves C_{2v} symmetry, and in the positive phase of this distortion one C–C bond lengthens and two others shorten, each by half as much. The positive phase stabilizes the $^1E_y'$ ($^1A_1$) component of $^1E'$ in both first and second order, while the negative phase stabilizes $^1E_x'$ ($^1B_2$), but only in first order. It is for this reason that one of the three equivalent minima on the potential surface for pseudorotation in planar cyclopropenyl anion (and, of course, in the isoelectronic $(NH)_3^{2+}$ as well) occurs for a positive e_y' distortion and that one of the three saddle points between minima is found along negative e_y'.

Distortions of both the N–H and N–N bond lengths were investigated in $(NH)_3^{2+}$. It was found that with all N–N bond lengths held equal, different N–H bond length distortions selectively stabilized one of the two components of $^1E'$. However, the stabilization energies were only on the order of 0.1 kcal/mol. Therefore, throughout the remainder of the calculations the N–H bonds were all fixed at 1.106 Å, the optimum D_{3h} value. The N–H bonds were assumed to bisect the N–N–N bond angles to further simplify geometry searches at non-D_{3h} molecular symmetries. With these constraints e_y' distortions of the N–N bonds were investigated, both at the SCF and at the CI level.

Shown in Figure 1 is the behavior of the $^1A_1$ MCSCF and $^1B_2$ RHF energies on negative e_y' distortion of the N–N bond lengths

---

(20) Jahn, H. A.; Teller, E. *Proc. R. Soc. London, Ser. A* **1937**, *161*, 220.

(21) For a lucid discussion of the second-order Jahn–Teller effect and leading references see: Pearson, R. *J. Am. Chem. Soc.* **1969**, *91*, 4947.

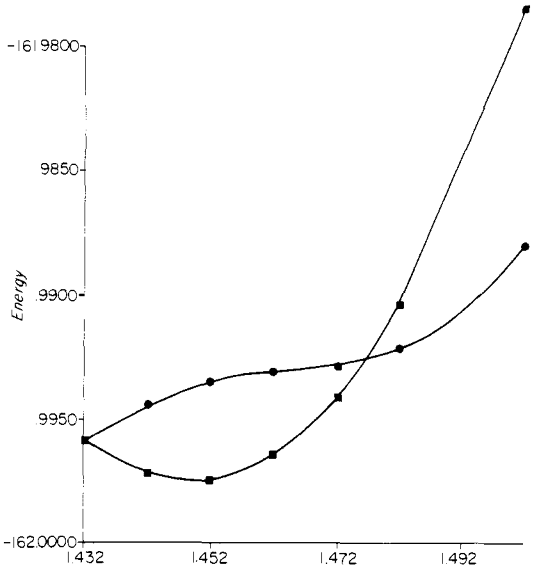

Figure 2. Energies of $^1A_1$ (●) and $^1B_2$ (■) σ–π CI wave functions (obtained with $^3B_2$ RHF MO's) on negative e_y' distortions from r_{N-N} = 1.432 Å. For such distortions $r_{N_1-N_2} = r_{N_1-N_3} = 2.148 - {}^1/_2 r_{N_2-N_3}$.

away from a common value of 1.432 Å. The curves for the π CI wave functions are very similar, since π CI has no effect on $^1B_2$ and only a very small effect on $^1A_1$. Although, as expected, $^1B_2$ is stabilized on negative e_y' distortions, $^1A_1$ is also stabilized on this phase of the distortion. Not only is $^1A_1$ stabilized on the "wrong" phase of distortion but its equilibrium distortion is smaller than that of $^1B_2$, and $^1A_1$ is less stabilized by distortion than is $^1B_2$. All of these features of Figure 1 are the opposite of what is expected, based on consideration of Jahn–Teller effects for $^1E'$ wave functions.[1] Of course, it should be recalled the neither SCF nor π CI calculations yield singlet wave functions of pure $^1E'$ symmetry in $(NH)_3^{2+}$. Therefore, there is no requirement that the SCF or π CI wave functions should behave as predicted for the components of $^1E'$. The results displayed in Figure 1 emphasize the importance of obtaining wave functions that exhibit the proper D_{3h} degeneracy. If the $^1A_1$ and $^1B_2$ wave functions do not exhibit D_{3h} degeneracy, not only will they obviously fail to have the correct relative energies at non-D_{3h} geometries but also the behavior of the individual energies on distortion may be qualitatively incorrect. Thus, the D_{3h} degeneracy of two wave functions that are purported to represent the two components of a $^1E'$ state should be viewed as a sine qua non for their acceptability.

The σ–π CI wave functions based on the $^3B_2$ RHF MO's do, of course, exhibit the proper D_{3h} degeneracy. The potential curves for these wave functions on negative e_y' distortions are shown in Figure 2. As should be the case, based on the analysis of the Jahn–Teller effects, the $^1A_1$ wave function is now stabilized on positive e_y' distortions, and its minimum occurs farther along this distortion coordinate ($r_{N_1-N_2} = r_{N_1-N_3}$ = 1.354 Å, $r_{N_2-N_3}$ = 1.588 Å) and at lower energy (−162.0114 hartree) than does the $^1B_2$ minimum along negative e_y'.

In addition to the qualitative differences between Figures 1 and 2, there is a quantitative difference in the position of the $^1B_2$ minimum on distortion. Upon inclusion of CI in the σ space, the magnitude of the distortion and the energy lowering produced by it are seen to decrease for $^1B_2$. As noted above, the distortion of $^1B_2$ along negative e_y' is entirely a first-order effect, caused by the deviation of the overlap populations in $^1B_2$ from D_{3h} symmetry at D_{3h} geometries. The overlap populations in both components of $^1E'$ have lower than D_{3h} symmetry, since the optimal MO's for each of them differ from those of $^3A_2'$. The $^3A_2'$ MO's are nonoptimal for $^1E'$ because the open-shell electrons in the singlet are not prevented by the Pauli principle from occupying the same region of space. The optimal MO's for the singlet tend to confine the two open-shell electrons to different regions of space, thus minimizing the ionic terms in the π wave function.

The reduced importance of the first-order Jahn–Teller effect on inclusion of σ–π CI suggests that the deviation of the overlap populations from D_{3h} symmetry is lessened in going from SCF (or π CI) to σ–π CI wave functions. This deduction is confirmed by comparison of the population analyses. The smaller difference between singlet and triplet wave functions on inclusion of CI in the σ space supports the contention that σ–π correlation stabilizes ionic terms in π wave functions.[22]

Since $^1B_2$ profits only from first-order Jahn–Teller stabilization, while $^1A_1$ benefits from both first-order and second-order effects, the relative importance of the two effects is readily obtained. The first-order effect stabilizes $^1B_2$ by 1.0 kcal/mol, while the combination of first- and second-order effects lowers the energy of $^1A_1$ by 9.6 kcal/mol. Thus, the second-order effect is certainly much more important than the first-order one. The dominance of the second-order effect in antiaromatic annulenes now seems firmly established,[9,18] although in diradicals like trimethylenemethane, where the atoms spanned by the open-shell MO's are not nearest neighbors, the first-order effect is the more important.[17]

The operation of both the first- and second-order Jahn–Teller effects on the $^1A_1$ state may be clearly seen in Figure 2. On negative e_y' distortion, the initial increase in energy is nearly linear, due to the dominance of the first-order effect for small distortions. Unlike the first-order effect, the second-order is quadratic in the distortion and thus stabilizes $^1A_1$ for both positive and negative e_y' distortions. It is apparent from the initial downward curvature of the $^1A_1$ energy on negative e_y' distortion that the magnitude of the second-order effect is sufficiently large to make the second derivative of the energy with respect to distortion positive. However, only the leading term in the perturbation expansion of the energy change resulting from $^1E_y'$–$^1A_1'$ mixing on e_y' distortion is quadratic. The second term in the expansion is quartic and has the opposite sign from the quadratic one. Therefore, for sufficiently large distortions the quartic term dominates. Consequently, a point of inflection is observed in the $^1A_1$ energy curve where the second derivative changes sign.

The operation of the second-order effect on $^1A_1$ for negative e_y' distortions keeps the energy of this state close to that of $^1B_2$, and ultimately they cross. At the crossing point a distortion that allows the mixing of these two states must result in an energy lowering that is linear in the distortion coordinate. This may be regarded as an "accidental" first-order Jahn–Teller effect,[23] in order to distinguish it from one that is due to a symmetry-enforced degeneracy. Even at points somewhat removed from the actual crossing, the mixing of the $^1A_1$ and $^1B_2$ states should result in a second-order energy lowering, due to the proximity of the unmixed states. The distortion required for mixing of these two states is one that leaves only the molecular plane as a symmetry element. Such a geometric distortion fom C_{2v} symmetry is required in order for a molecule on the negative e_y' axis to reach one of the two minima, symmetrically disposed about e_y', that are equivalent to the third that lies along positive e_y'. Thus, the second-order effect that stabilizes $^1A_1$ serves not only to create minima on the potential surface for pseudorotation but also to favor at the saddle points the type of molecular distortions that will channel molecules down toward the minima.

σ–π CI energies were also computed at C_{2v} geometries by using the orbitals from $^1A_1$ MCSCF and $^1B_2$ RHF calculations. The behavior of the $^1A_1$ and $^1B_2$ σ–π CI energies on e_y' distortions was qualitatively similar to that found when $^3B_2$ RHF MO's were used, except that the energy of $^1A_1$ on negative e_y' distortion rose more steeply than when the $^3B_2$ RHF MO's were employed. At all points investigated on the energy surface for planar $(NH)_3^{2+}$ the σ–π CI energies based on $^3B_2$ MO's were found to be lower than those obtained with $^1A_1$ or $^1B_2$ MO's. The triplet MO's, of course, have the additional virtue of giving a pure $^1E'$ pair of wave functions at D_{3h} geometries and hence are obviously the MO's

---

(22) See ref 18 and citations therein.

(23) For a discussion of "accidental" Jahn–Teller effects see: Davidson, E. R. *J. Am. Chem. Soc.* **1977**, *99*, 397; Davidson, E. R.; Borden, W. T.; Smith, J. *Ibid.* **1978**, *100*, 3299.

Table II. Results of Modified CI Calculations[a] on $(NH)_3^{2+}$

state	type of geometry	$r_{N_1-N_2}$,[b] Å	$r_{N_2-N_3}$, Å	ϕ_1, deg	ϕ_2,[c] deg	energy, hartrees
$^1E'$ [d]	$^1E'$ D_{3h} minimum	1.442	1.442	0	0	−161.9525
$^1B_2$ [e]	$^1E'$ D_{3h} minimum	1.442	1.442	0	0	−161.9532
$^1A_1$ [f]	$^1E'$ D_{3h} minimum	1.442	1.442	0	0	−161.9509
$^3A_2'$ [d]	planar minimum	1.421	1.421	0	0	−162.0060
$^1A_1$ [f]	$^1A_1$ C_{2v} minimum[g]	1.340	1.641	0	0	−161.9644
$^1B_2$ [e]	$^1B_2$ C_{2v} minimum[h]	1.459	1.405	0	0	−161.9550
$^1A'$ [d]	global minimum[i,j]	1.622	1.279	74.7	−2.9	−162.0456
$^1A'$ [f]	saddle point[k,l]	1.375	1.675	3.6	−51.0	−162.0084
$^3A''$ [d]	triplet global minimum[m]	1.457	1.451	43.5	−40.3	−162.0279
^3B [d]	triplet saddle point	1,434	1.478	0	43.2	−162.0217
^1B [d]	excited singlet global minimum[h,n]	1,476	1.482	0	54.3	−161.9835
$^1A''$ [e]	excited singlet saddle point[h]	1,477	1.446	37.1	−41.2	−161.9779

[a] See text for a description. [b] This bond length is the same as that between N_1 and N_3. [c] This out-of-plane hydrogen bending angle is the same as that at N_3 for A' and A'' states (C_s symmetry) and has the same magnitude but opposite sign for A and B states (C_2 symmetry). [d] Computed with $^3A''(^3B)$ MO's. [e] Computed with $^1A''(^1B)$ MO's. [f] Computed with $^1A'(^1A)$ MO's. [g] With $^3A''$ MO's the optimal distortion from D_{3h} symmetry was smaller by about 0.03 Å for the two equivalent bonds and 0.06 Å for the unique bond, but the CI energy at the minimum was only 0.0004 hartree higher. [h] With $^3A''(^3B)$ MO's the optimal geometry and the CI energy were very similar to those found with $^1A''(^1B)$ MO's. [i] The $^1A'$ MO's gave bond lengths for the global $^1A'$ minimum that were less distorted from D_{3h} symmetry and a CI energy that was somewhat higher. [j] The energy at the planar geometry with these bond lengths was −161.9182 hartree; therefore nitrogen pyramidalization results in a vertical stabilization of 0.1274 hartree (80.0 kcal/mol). [k] As at planar geometries, $^3A''$ MO's gave optimal bond lengths that were less distorted from their D_{3h} values and a slightly higher CI energy at the optimal geometry. [l] The energy at the planar geometry with these bonds lengths was −161.9615 hartree; therefore nitrogen pyramidalization results in a vertical stabilization of 0.0469 hartree (29.4 kcal/mol). [m] The energy at the planar geometry with these bond lengths was −162.0031 hartree; therefore nitrogen pyramidalization results in a vertical stabilization of 0.0248 hartree (15.6 kcal/mol). [n] The energy at the planar geometry with these bond lengths was −161.9496 hartree; therefore nitrogen pyramidalization results in a vertical stabilization of 0.0339 hartree (21.3 kcal/mol).

of choice for carrying out $\sigma-\pi$ CI on the singlet states of planar $(NH)_3^{2+}$, at least with a minimal basis set.

Nevertheless, it should be stressed that, unlike the two-configuration MCSCF or π CI calculations on $^1A_1$, all the $\sigma-\pi$ CI calculations find $^1A_1$ to distort along positive, rather than negative, e_y'. For positive e_y' distortions, which lengthen one bond and shorten the other two, the π wave function for $^1A_1$ prefers the orbital occupancy $1b_1^2a_2^2$. The orbitals resemble those occupied in an allyl anion-like wave function (e.g., **2**). The virtual $2b_1$ orbital is used to correlate the electrons in the allyl nonbonding a_2 MO. For negative e_y' distortions the preferred orbital occupancy is $1b_1^22b_1^2$. These are the orthogonalized orbitals for an ethylenic π bond and a nonbonding p orbital on the unique atom, as in **1**. The a_2 virtual orbital is used to correlate the pair of ethylenic π electrons. Correlation of this pair of electrons requires little shift in π charge. In contrast, correlation of the a_2 pair in a wave function resembling an allylic anion entails a significant shift of π charge because a_2 is confined exclusively to the two terminal atoms, while the virtual $2b_1$ orbital has substantial density on the central atom. Consequently, when the σ core is frozen, the π wave function is biased toward a $1b_1^22b_1^2$ orbital occupancy, since essentially the same set of σ orbitals is appropriate for this configuration and for the one that is most important in providing correlation for it. A manifestation of this fact is that at a D_{3h} geometry, where $1b_1^22b_1^2$ and $1b_1^2a_2^2$ should have equal weights, the coefficient of the former is 0.84 while that of the latter is 0.54 in both the MCSCF and π CI wave functions. Since the MCSCF and π CI $^1A_1$ wave functions prefer $1b_1^22b_1^2$ over $1b_1^2a_2^2$ at D_{3h} geometries, it is not surprising that both MCSCF and π CI $^1A_1$ wave functions favor distortion along negative e_y' to geometries more appropriate for the former configuration.

When flexibility is introduced into the σ wave function, by allowing for single σ valence excitations from all possible π configurations, in the CI expansion for $^1A_1$ the coeficients of the dominant terms involving $1b_1^22b_1^2$ and $1b_1^2a_2^2$ π configurations become essentially equal at D_{3h} geometries. The next largest coefficient belongs to $1b_12b_1a_2^2$, an excitation that alters the $1b_1$ orbital in $1b_1^2a_2^2$ from the MCSCF $1b_1$ MO.[24] Single excitations that modify the σ cores of $1b_1^2a_2^2$ and $1b_12b_1a_2^2$ from that of $1b_1^22b_1^2$ also have large (>0.1) coefficients. It is the latter terms that prevent the $^1A_1$ wave function from being spuriously biased toward that for a π bond plus a localized lone pair of electrons, with a concomitant and equally spurious bias toward a preferred molecular geometry with one short and two long bonds. This is why $\sigma-\pi$ CI is essential for obtaining $^1A_1$ wave functions that show the correct preference for molecular geometries involving positive e_y' distortions.

Calculations at Nonplanar Geometries. Having discovered a CI methodology that gives a satisfactory description of planar $(NH)_3^{2+}$, we wished to extend our calculations to nonplanar geometries, since, as indicated in the introduction, at least some of the states of this molecule could reasonably be expected to prefer such geometries. However, our CI prescription, calling for the generation of all configurations in which a single σ valence electron is excited into a virtual σ orbital for all possible π configurations, obviously relies on $\sigma-\pi$ separability. Since the distinction between σ and π orbitals is lost at nonplanar geometries, we were forced to modify somewhat our CI protocol.

We reasoned that, on nitrogen pyramidalization, the strongest $\sigma-\pi$ mixing would involve the occupied Walsh orbitals of the three-membered ring,[25] which are the highest energy filled σ MO's. SCF calculations supported this supposition. Therefore, we included in our modified CI all the possible configurations formed by distributing ten electrons among the six occupied SCF orbitals of highest energy. At planar geometries these six orbitals correspond to the three π and the three filled Walsh MO's. Single excitations from these six orbitals into the four virtual orbitals of lowest energy were allowed for all these configurations. In order to keep the modified CI about the same size as that used for planar geometries, where $\sigma-\pi$ separability could be capitalized upon, the two highest energy virtual MO's were not included in the modified CI. This prescription was used to generate singlet configurations belonging to the A′ representation of the C_s point group (A in C_2) and singlet and triplet configurations belonging to A″ (B in C_2). This resulted in 153 $^1A'$ (^1A) space–spin product configurations, 148 $^1A''$ (^1B), and 188 $^3A''$ (^3B).

At planar geometries many of these configurations do not contribute, because they involve $\sigma-\pi$ excitation of a single electron. Since in C_{2v} symmetry these configurations consequently have B_1 or A_2 symmetry, they do not mix into the A_1 and B_2 wave functions. As a result of the fact that the modified CI at planar geometries is thus smaller than the previous one involving *all* single σ valence excitations for every π configuration, the energies ob-

---

(24) The $1b_12b_1a_2^2$ configuration also provides interorbital correlation for $1b_1^22b_1^2$, but the coefficient of $1b_12b_1a_2^2$ is more than a factor of 10 larger when σ CI is included than when just π CI is carried out.

(25) Walsh, A. D. *Nature (London)* **1947**, *159*, 712.

tained with the modified CI are each about 0.04 hartree higher. The D_{3h} energies at an N–N bond length of 1.442 Å, which is optimal for the $^1E'$ state,[26] are shown in Table II. Because the modified CI provides a less flexible σ core than the previous CI protocol, the energy of $^1E'$ that is obtained with the $^3A_2'$ MO's, now lies between those of the $^1A_1$ and $^1B_2$ components that are calculated, respectively, with $^1A_1$ MCSCF and $^1B_2$ RHF MO's.

The similar energies of the two lowest singlet states at D_{3h} geometries, whether or not D_{3h}-symmetry orbitals are used to carry out the CI, provide one measure of the adequacy of the modified CI method. Another indication of its adequacy is the behavior of the $^1A_1$ and $^1B_2$ wave functions on distortion to C_{2v} geometries. As expected from the Jahn–Teller considerations discussed above, $^1A_1$ is found to distort farther along positive e_y' and shows a greater energy lowering on this distortion that does $^1B_2$ along negative e_y'. The results of the calculations at C_{2v} geometries, summarized in Table II, are similar to those obtained with the previous σ–π CI method.

With the adequacy of our modified CI prescription established at planar geometries, we proceeded to use it to carry our CI calculations at the nonplanar geometries for which it was designed. Only geometries that preserved either a plane or axis of symmetry were investigated. This simplifying constraint on geometry searches was based on the reasonable assumption that the maxima and minima on the global energy surfaces for $(NH)_3^{2+}$ would involve species with e_y'-distorted bond lengths that had undergone out-of-plane hydrogen bending, belonging to either the b_1 or a_2 representations of C_{2v}. At nonplanar geometries the remaining symmetry element, a plane or an axis, was employed to partition the MO space in the SCF calculations and the configuration space in the CI calculations that followed. The MO basis that gave the lowest CI energy was used to optimize each geometry for each state.

Geometry optimizations for the lowest singlet state were begun at the C_{2v} minimum of $^1A_1$ and near the point of inflection shown in Figure 2 for this state. The hydrogen out-of-plane bending angle (or angles) that least disrupted bonding π interactions between nitrogens was optimized first, followed by the longest N–N bond length(s), then the remaining bond distance(s), and finally the second out-of-plane angle(s). Another complete cycle of optimization was then carried out.

Since $^1A_1$ distorted along negative e_y' contains a strong ethylenic π bond, as in **1**, appreciable nonplanarity of the two nitrogens forming this π bond seemed most unlikely. Therefore, C_2 geometries, which involve pyramidalization of only these two nitrogens, were not investigated for negative e_y'-distorted bond lengths in this state. A C_2 geometry is certainly a possibility for $^1A_1$ with two short N–N bonds and one long one as in **2**. However, for positively distorted e_y' bond lengths in $^1A_1$, pyramidalization of the two relevant nitrogens was found to occur preferentially syn rather than anti, leading to a geometry of C_s, instead of C_2 symmetry. It should be noted, however, that MCSCF convergence problems for ^1A wave functions at C_2 geometries kept us from obtaining a fully optimized structure of this type. Thus, although we certainly believe the preferred geometry for the lowest singlet state with two long N–N bonds and one short one has C_s symmetry, we cannot completely rule out the possibility that a fully optimized C_2 structure might have lower energy. The optimized C_s geometries for $^1A_1$ are given in Table II. On the basis of additional calculations around these geometries, obtained after two cycles of optimization, the out-of-plane bending angles appear to be within 1° and the bond lengths within a few thousandths of an angstrom of their optimal values.

It seemed likely that since planar $^3A_2'$ prefers a D_{3h} geometry, the bonds would still be close to the same length, even after nitrogen pyramidalization. Therefore, in optimizing the geometry of the triplet state, both sets of out-of-plane bending angles were first optimized, followed by the bond lengths. Another cycle of geometry optimization was then carried out. As shown in Table II, both a C_s and a C_2 structure were found.

A C_s and a C_2 structure were also found for the remaining singlet state, using the same optimization cycle employed for the triplet. However, after one cycle of optimization, it was clear that this open-shell singlet, $^1A''$ at C_s geometries and ^1B at C_2, would lie above the closed-shell singlet at all nonplanar geometries. Therefore, a second cycle of optimization was not carried out for this excited singlet state. The geometries reported in Table II for this state are, consequently, less likely to be optimal than are the geometries for the lowest singlet and triplet states.

Discussion

Perhaps the most surprising feature of the results contained in Table II is that all three low-lying states of $(NH)_3^{2+}$ prefer highly nonplanar geometries. While both singlet states might have been expected to undergo nitrogen pyramidalization in order to relieve localized antibonding π interactions, the fact that this type of distortion is also favorable for the fully delocalized $^3A_2'$ state warrants some comment.

Nitrogen pyramidalization in $(NH)_3^{2+}$ may be viewed as a second-order Jahn–Teller effect in which the lowest state of the planar species is mixed by an out-of-plane vibration with excited states in which a π electron is transferred into a virtual σ orbital.[21,27,28] Pyramidalization will be most favored if there is such an excited state close to the ground state in energy, a circumstance that is most likely to obtain in a molecule containing a π orbital that is relatively high in energy and an unfilled σ antibonding orbital that is relatively low. The highest filled π orbital in all the states of planar $(NH)_3^{2+}$ is antibonding in nature. It has previously been pointed out that small rings contain low-lying unfilled σ orbitals, whose presence is responsible for the fact that pyramidalization of ring atoms with unshared electrons is strongly favored in such molecules.[27] Therefore, it is not so very surprising that all the states of $(NH)_3^{2+}$ are found to undergo second-order Jahn–Teller distortions to nonplanar geometries.

What makes the pyramidalization in $^3A_2'$ somewhat unexpected is that π bonding obviously must be sacrificed. For the same reason the pyramidalization of the $^1B_2$ state at the two equivalent nitrogens between which there exists π bonding appears strange, until it is recalled that the highest energy MO in this state—the singly occupied ethylenic antibonding, π orbital—spans these two atoms.

Nevertheless, one's intuition that, other things being equal, pyramidalization at an atom not involved in π bonding should be more favorable than pyramidalization at one that is, is amply borne out. The wave function that is most stabilized by nitrogen pyramidalization resembles that for **1** and consists of essentially an ethylenic π bond and a pair of electrons localized at the third nitrogen. Pyramidalization at the unique nitrogen destroys no π bonding; on the contrary, it might be expected to mitigate the antibonding interaction between the lone pair on this nitrogen and the ethylenic π bond. This supposition is confirmed by population analyses.[29]

Population analyses confirm another expectation. Pyramidalization of the two terminal nitrogens at positive e_y'-distorted geometries is even more important in partially relieving the very

---

(26) It should be noted that the optimal D_{3h} bond lengths for both $^1E'$ and $^3A_2'$ are longer than those obtained with the previous CI prescription and reported in Table I. This result is due to the fact that, although the modified CI is smaller at planar geometries, it does allow for the inclusion of configurations in which two electrons are excited from bonding Walsh σ orbitals into antibonding π orbitals. Inclusion of these configurations lowers the energy by providing additional correlation for the σ electrons; however, the presence of these configurations also reduces the N–N overlap populations thus leading to longer optimal bond lengths.

(27) Cherry, W.; Epiotis, N.; Borden, W. T. *Acc. Chem. Res.* **1977**, *10*, 167.

(28) The theory of the second-order Jahn–Teller effect can be used to predict the preferred mode of pyramidalization when a molecule contains two or more centers at which pyramidalization can occur. Volland, W. V.; Davidson, E. R.; Borden, W. T. *J. Am. Chem. Soc.* **1979**, *101*, 533. Strozier, R. W.; Caramella, P.; Houk, K. N. *Ibid.* **1979**, *101*, 1340.

(29) The overlap matrix between the atoms was diaganolized in order to partition the overlap populations between atoms into "σ" and "π" components at nonplanar geometries. The "π" orbitals were taken to be those p functions orthogonal to the plane containing the three nitrogens.

substantial antibonding π interaction between these centers in the $^1A_1$ wave function, which resembles that for **2** at such geometries. The existence of the antibonding interaction is manifested by the very long bond between N_2 and N_3. However, pyramidalization of these two nitrogens also diminishes the π bonding between them and the central nitrogen. Thus $^1A_1$ profits much more from pyramidalization of one nitrogen at negative e_y'-distorted geometries than from pyramidalization of two nitrogens at positive e_y'-distorted geometries.[30]

Although the population analyses do reveal the expected reductions in the magnitude of π interactions on nitrogen pyramidalization, the size of these changes is much smaller than many others that occur in the density matrix.[31] For instance, in planar $^1A_1$ with the same negatively e_y'-distorted bond lengths as at the global minimum, the π-bond order between the unique nitrogen and each of its neighbors is -0.118. At the global singlet minimum, where the unique nitrogen is highly pyramidalized, the π-bond order is -0.088. However, the σ-bond order between the unique nitrogen and each of its neighbors changes from 0.366 to 0.244 on pyramidalization, 4 times as much. The change in the σ overlap population (the product of bond order and overlap) is 20 times that in the π, since the σ overlap integral is 5 times the size of the π.

The σ overlap populations are reduced in all the other low-lying states too by nitrogen pyramidalization. This fact is manifested not only in the population analyses but also in the occurrence of the nonplanar minima at longer N–N bond lengths than their planar counterparts. The reduction in the σ overlap populations contradicts the commonly held belief that the driving force for pyramidalization of atoms in small rings is the relief of "strain" in the σ ring bonds by atom rehybridization. Therefore, one is led to ask just what it is that makes nitrogen pyramidalization so energetically favorable in $(NH)_3^{2+}$.

The theory of the second-order Jahn–Teller effect provides a simple answer to this question. In orbital terms pyramidalization allows the mixing of the high-lying filled π MO's with the low-lying empty σ orbitals in $(NH)_3^{2+}$, and it is precisely this mixing that provides the driving force for pyramidalization.

The lowest unfilled σ orbitals are both N–N and N–H antibonding in character. They are low in energy because they contain large contributions from the nitrogen 2s orbitals, whose utilization in N–N bonding MO's is inhibited by the small bond angles in the three-membered ring. The admixture of one of these antibonding σ orbitals to the wave function has a number of effects, all of which are visible in the comparison of the population analyses for planar and nonplanar geometries.

First, since these unfilled σ orbitals are N–N antibonding, the N–N σ-bond orders are reduced, as discussed above. It might be imagined that, because of the large antibonding interaction between N-2s and H-1s AO's in the unfilled σ MO's, the N–H bond orders would also be reduced. However, this is not the case. The bonding interaction between the hydrogen 1s AO's in the unfilled σ MO's and the nitrogen 2p orbitals in the filled π MO's is what results in the mixing of these MO's. This bonding interaction mitigates the decrease in N–H bonding caused by putting electron density into orbitals that are N–H antibonding. In fact, population analyses show that the N–H overlap populations are almost unchanged on nitrogen pyramidalization, although the character of the N–H bonds is greatly altered.

The alteration in the character of the N–H bonds is the second major change that occurs on nitrogen pyramidalization. Since the filled π orbitals are confined exclusively to nitrogen atoms, while the unfilled σ orbitals have significant contributions from hydrogen 1s orbitals, there is a flow of charge from nitrogen to hydrogen on pyramidalization. For instance, in the $^1A_1$ wave function that resembles **1**, with a lone pair of electrons essentially localized on the unique nitrogen, the gross electron population on this nitrogen decreases from 7.11 to 6.72 on pyramidalization. This decrease is due to a drop in the π population on this atom from 1.98 to 1.49. The gross population at the unique hydrogen increases from 0.36 to 0.61, and the other two nitrogens each gain about 0.05 electrons. These nitrogens gain electron density because the π lone-pair orbital is largely localized at the unique nitrogen, while the low-lying σ orbital that is mixed with it has contributions from these two nitrogen atoms. Although the overlap population in the unique N–H bond increases from 0.23 to 0.26, the nitrogen 2s contribution to it drops from 0.15 to less than 0.02, because of the large 2s–1s antibonding component in the virtual σ MO.

It should be noted that these changes are exactly what is expected if the unique nitrogen undergoes a change in hybridization on pyramidalization so that the amount of 2s character it uses in all its bonds, but particularly in the bond to hydrogen, is reduced. Since 2s orbitals are lower in energy and hence more electronegative than 2p orbitals, the more 2s character that an atom uses in a bond, the more it will pull electron density toward it. For instance, at the unique nitrogen in the optimal geometry for the $^1A_1$ wave function that resembles **1** the N–N–N bond angle is only 46.5°. Consequently, one would expect the unique nitrogen in the planar molecule to use less s character in its N–N bonds and more s character in its N–H bond than the other two nitrogens. In fact, the nitrogen 2s contribution to the N–H overlap population in the planar molecule is almost 50% larger for the unique N–H bond than for the other two. Therefore, the unique N–H bond should be strongly polarized toward nitrogen.[32] Indeed, despite the fact that the population analysis finds the unique nitrogen to be negatively charged in the planar molecule, the population at the attached hydrogen (0.36) is actually less than that (0.50) at each of the two equivalent hydrogens. However, on pyramidalization of the unique nitrogen, rehybridization occurs and the 2s contribution to the N–H overlap population is reduced by almost an order of magnitude, as noted above. Consequently, after pyramidalization the electron population at the unique hydrogen (0.61) actually exceeds that at each of the two equivalent hydrogens, whose populations remain essentially unchanged.

Both the second-order Jahn–Teller analysis and the hybridization-based perspective make the same prediction regarding the third important change that takes place on pyramidalization, namely, the alteration of the character of the orbitals occupied by the π electrons in the planar molecule. These pure 2p orbitals are expected to acquire appreciable 2s character. That this change does occur is manifested in the fact that at the geometry corresponding to the global minimum, although the 2s contribution to the unique N–H bond drops by almost an order of magnitude on pyramidalization of the unique nitrogen, the gross electronic population in the 2s orbital on this nitrogen actually increases from 1.64 to 1.89. In the Jahn–Teller analysis the increase in the gross 2s population at this nitrogen is a natural consequence of the fact that electrons are being partially removed from a filled orbital that is pure 2p and being placed in one that has substantial 2s character at nitrogen. From a rehybridization perspective, the increase in 2s population at the unique nitrogen can be viewed as a consequence of the fact that the pair of electrons in the N–H bond is shared between nitrogen and hydrogen, while the lone pair is localized on nitrogen. Thus, on pyramidalization, 2s character

---

[30] The greater stabilization on ring atom pyramidalization of the wave function represented by **1**, compared to the one portrayed by **2**, is nicely predicted by a second-order Jahn–Teller analysis. Focusing on stabilization of the highest occupied MO (HOMO) in each of the two π wave functions, it is easy to show that the two equivalent atoms in **2** must *each* pyramidalize by the same amount as the unique atom in **1**, in order to provide roughly the same amount of second-order stabilization. Since pyramidalization of two atoms by θ represents a distortion $2^{1/2}$ times that resulting from pyramidalization of just one atom by this amount, pyramidalization of the unique atom in **1** is predicted to afford about twice as much stabilization for each unit of distortion as pyramidalization of the two equivalent atoms in **2**. To the extent that the lowest π MO in **2** also mixes with unfilled σ orbitals on pyramidalization, thus entailing a loss of π bonding, focusing only on the HOMO's represents, of course, an oversimplification.

[31] Since comparisons between planar and nonplanar geometries were made by using the same set of bond lengths, the atomic overlaps between bonded atoms are identical in the two geometries. Therefore, the overlap populations are in the same ratio as the elements of the density matrix.

[32] This is why substituents that are less electronegative than hydrogen are found to stabilize strained rings. Dill, J. D.; Greenberg, A.; Liebman, J. F. *J. Am. Chem. Soc.* **1979**, *101*, 6814.

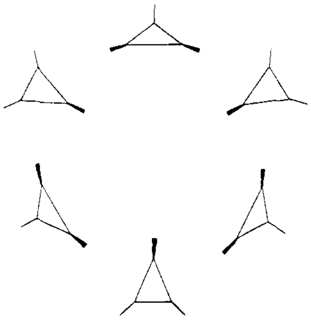

Figure 3. Schematic depiction of pseudorotation in the lowest singlet state of $(NH)_3^{2+}$. The heavy lines represent N–H bonds that lie appreciably above the N–N–N plane.

is being removed from an orbital that is only partially confined to nitrogen and being added to an orbital that is completely localized at this atom, thereby increasing the electron population in the nitrogen 2s orbital.

The population analyses at the minima for all the low-lying states of $(NH)_3^{2+}$ reveal an increase in the 2s populations of the nitrogens that are pyramidalized. In the rehybridization model it is this effect, not a relief of strain in the σ bonds of the ring, that provides the driving force for pyramidalization. The large amount of 2s character that is present in the exocyclic bonds of the planar strained ring can be more effectively used to stabilize electrons that are nonbonding or that participate only in weak π bonding. The larger the π-electron density at a particular nitrogen and the weaker the π bonding involving that nitrogen, the greater the driving force for pyramidalization of that nitrogen.

Since the $^1A_1$ wave function at negative e_y'-distorted geometries has a pair of nonbonding (or, more precisely, slightly antibonding) π electrons localized at a single nitrogen, it is not at all surprising that this state profits most from a distortion to a nonplanar geometry. As shown in Figure 2, this type of wave function (**1**) is not even a secondary minimum on the energy surface for the planar molecule. However, Table II reveals that on pyramidalization of the unique nitrogen, the energy of this type of wave function falls well below that corresponding to the $^1A_1$ planar minimum (**2**) with the two equivalent nitrogens pyramidalized.

The latter species is a saddle point on the global surface. It is a transition state on the pseudorotation pathway connecting the two other equivalent $^1A'$ global minima. Pseudorotation in the lowest singlet state of $(NH)_3^{2+}$ is illustrated in Figure 3. Because of the large calculated energy difference between the minima and transition states (23.3 kcal/mol), pseudorotation in the lowest singlet state is predicted to be a relatively slow process, one that could easily be frozen out on the NMR time scale. Since the singlet is indicated by the calculations to be the ground state of the molecule, the prediction of slow pseudorotation in this state should be readily testable.

The triplet with its fully symmetrical π bonding and π-electron density is able to profit much less from nitrogen pyramidalization than the lowest singlet state. Consequently, although the triplet is predicted to be the ground state of planar $(NH)_3^{2+}$, nitrogen pyramidalization causes the lowest singlet to fall below the triplet in energy. On the global triplet surface the stationary points with C_s symmetry are minima, and those with C_2 are transition states on a pseudorotation pathway connecting the minima.[33] However, pseudorotation is predicted to be relatively facile in the triplet state, requiring only 3.9 kcal/mol for activation. Facile pseudorotation is also predicted in the lowest singlet excited state,[33] although the roles played by the stationary points of C_s and C_2 symmetry are reversed from the triplet state.

Conclusions

Three types of conclusions can be drawn from this study. The first of these is methodological. We have shown that σ–π CI is essential for correctly describing molecules in which a nonuniform distribution of π charge results in a complementary distortion of the electron density in the σ core.[35] The required σ–π coupling at the CI level should deter future attempts to use π-electron methods,[36] SCF, or even SCF followed by π CI for studying such systems.

The second type of conclusion regards the driving force for pyramidalization of atoms with π electrons in small rings. Our results on $(NH)_3^{2+}$ show that pyramidalization does not result from relief on strain in the ring bonds; in fact, the σ overlap populations between nitrogens in $(NH)_3^{2+}$ decrease on pyramidalization. Instead, pyramidalization results from the utilization of the appreciable 2s character in the bond exocyclic to the ring for the stabilization of the electrons that occupy a pure π orbital in the planar molecule. The electronic changes that occur on pyramidalization are all very nicely described by the formalism of second-order Jahn–Teller effects.

Finally, our calculations predict that $(NH)_3^{2+}$ should be a ground-state singlet in which two nitrogens form an ethylenic π bond and the unique nitrogen, bearing a lone pair of electrons, is highly pyramidalized. Pseudorotation between the three equivalent minima on the singlet surface is calculated to require substantial activation. Since our calculations were performed with a minimal basis set, the exact amount of energy actually required may be somewhat different from 23.3 kcal/mol computed.

Assuming that at least our qualitative findings on $(NH)_3^{2+}$ are substantiated by much more expensive σ–π CI calculations with a basis set of double-ζ quality that is augmented by polarization functions, one might hope that these results would have some relevance to the isoelectronic cyclopropenyl anion in solution. In particular, the prediction of a high activation energy for pseudorotation might be tested, at least in principle, by labeling the unique carbon in cyclopropene and determining whether scrambling of the label occurs upon base-catalyzed anion formation.

Unfortunately, even triphenylcyclopropene is so nonacidic that it does not undergo base-catalyzed hydrogen exchange.[5] Although diphenylcyclopropenyl cyanide does undergo base-catalyzed exchange, experiments with an optically active derivative show that racemization is competitive with exchange.[37] This finding suggests that the cyano group causes considerable flattening at the unique ring carbon, making a comparison with our calculations on $(NH)_3^{2+}$ meaningless.[38] Thus, it would appear that if our prediction of slow pseudorotation in the lowest singlet state of an annulene containing four π electrons in a three-membered ring is to be confirmed, $(NH)_3^{2+}$ or a simple derivative thereof may provide the best system for experimental scrutiny.

Note Added in Proof. In order to confirm the STO-3G prediction of a singlet ground state for $(NH)_3^{2+}$ with a substantial barrier to pseudorotation, we have carried out further CI calculations using a basis set of double-ζ quality, augmented by polarization functions.[39] Calculations were performed at the STO-3G geometries for the $^1A'$ global minimum and pseudoro-

---

[33] In states where stationary points of C_s and C_2 symmetry alternate along the pseudorotation coordinate, pseudorotation by 360° transforms the starting geometry into its mirror image. Pseudorotation by 720° is required to return to the original structure. This fact has a common topological origin with the observation that pseudorotation by 360° changes the sign of the electronic wave function for a three-atom, three-electron system.[34]

(34) Longuet-Higgins, H. C. *Proc. R. Soc. London, Ser. A* **1975**, *344*, 147.

(35) An analogous strong coupling between "valence" and "core" electrons is found in calculations on open-shell atoms. See, for instance: Weiss, A. W. *Adv. At. Mol. Phys.* **1973**, *9*, 1–46 and references therein.

(36) For an excellent discussion of π-electron calculations see: Parr, R. G. "Quantum Theory of Molecular Electronic Structure"; W. A. Benjamin: New York, 1963; pp 41–5.

(37) Breslow, R.; Douek, M. *J. Am. Chem. Soc.* **1968**, *90*, 2698.

(38) The calculations on the potential surface for *planar* $(NH)_3^{2+}$ might, however, bear on the behavior of cyclopropenyl anions whose planarity was favored by substituents with low-lying empty π orbitals. As noted by Breslow,[4] the pK_a of triphenylcyclopropene suggests that at least two of the phenyl groups are acting to stabilize the negative charge in the anion.

(39) The CI included all single and double excitations from the RHF wave function for the triplet and from the two-configuration MCSCF wave function for the singlet. The basis set and CI methodology are described in detail in: Feller, D.; Borden, W. T.; Davidson, E. R. *J. Chem. Phys.* **1979**, *71*, 4987.

tation transition state, the $^3A''$ global minimum, and the $^3A_2'$ planar minimum. The energies (hartrees), relative to that of the $^1A'$ global minimum (−164.4594), were as follows: $^1A'$ pseudorotation transition state (0.0419), $^3A''$ global minimum (0.0226), $^3A_2'$ planar triplet minimum (0.0424). The agreement between these results and those obtained with the STO-3G basis is very good; the largest discrepancy between relative energies is less than 0.005 hartree (3 kcal/mol). The extremely close correspondence between the two sets of calculations is actually somewhat surprising, since the STO-3G basis set overestimates the barrier to inversion in ammonia by about 5 kcal/mol[40] and this failing is apparently accentuated when CI is included.[41]

Acknowledgment is made to the donors of the Petroleum Research Fund, administered by the American Chemical Society, and to the National Science Foundation for support of this work.

---

(40) See, for instance, the tabulation in: Carlsen, N. R.; Radom, L.; Riggs, N. V.; Rodwell, W. R. *J. Am. Chem. Soc.* **1979**, *101*, 2233.

(41) Stevens, R. M. *J. Chem. Phys.* **1974**, *61*, 2086.

The Region of Mechanistic Transition in Acid-Catalyzed Epoxide Ring Opening. A Mechanistic Switch Mediated by Salt in Aqueous Media[1]

Y. Pocker* and B. P. Ronald[2]

Contribution from the Department of Chemistry, University of Washington, Seattle, Washington 98195. *Received August 20, 1979*

Abstract: The mechanism of the acid-catalyzed ring opening of tetramethylethylene oxide has been explored through ^1H NMR and UV spectrophotometric product analysis in aqueous media. In dilute aqueous media below pH 4 the hydrolysis proceeds to the extent of 99.92% forming pinacol; no detectable amount of pinacolone is formed from a possible rearrangement pathway. With increasing amounts of $NaClO_4$ at constant acid concentration there is a dramatic change in the products; rearrangement products appear even at 2.0 M aqueous $NaClO_4$, and rise to the extent of 10% at 6.0 M $NaClO_4$. Formate buffers in these salt solutions lead to the formation of pinacol monoformate ester concurrent with pinacolone and pinacol; however, limitations in the solubility of the epoxide substrate prohibited rate measurements. The dramatic product change arising from a novel salt effect in aqueous media reveals a mechanistic pathway switch for this acid-catalyzed epoxide ring opening. The initiating step in the mechanism with or without salt is the same, the formation of the protonated epoxide as an intermediate. Nucleophile-assisted opening of the intermediate by water or formate buffer uniquely excludes products derived from skeletal rearrangement. Howerver, high salt concentrations can provide the necessary electrostatic stabilization required for charged intermediates as well as reduce the probability of nucleophilic attack by water. The switch to a carbonium ion intermediate (a species isomeric with the protonated epoxide) is signaled by pinacolone formation.

The exploration and identification of the consequences of adding electrolyte to reaction media have received intensive exploration.[3a] Ingold and co-workers[3b] in an extensive series of studies showed that observations such as rate enhancement or retardation could be used to diagnose charge distribution in transition states in solvolytic reactions of organic halides and other substrates. Because of the low dielectric constant associated with many of the media in these studies, the exact state of the electrolyte remained in doubt. Winstein and co-workers[4] developed the ion-aggregate hypothesis for solvolytic reactions building on the results of data from Kolthoff et al.[5a] In media such as ethanol, acetic acid, formic acid, and acetone, as pure solvents, and when mixed with small quantities of water most salts are found in highly associated form. Certain salts, however, induce very interesting chemical effects arising from a low driving force for aggregate formation or because of selective solvation of one of the ions. Such salts give rise to the "special salt effect" characterized by Winstein et al.[4,5b,6] and to the phenomenon of "electrostatic catalysis" examined by Pocker et al.[7]

These effects are not generally observed in the study of organic reactions in purely aqueous media, as the extent of ionic aggregation is small even at modest concentrations of salt.[8] Indeed salts are often added to reaction systems in order to maintain a constant ionic strength in buffer catalysis studies. Recent examination of the acid-catalyzed epoxide ring-opening step shows that it proceeds with a significant contribution from mechanisms with S_N2 character.[9] We sought then a means of taking advantage of this unusual result by modifying the transition-state environment in an effort to observe a contribution to the ring opening from the S_N1 mode and the immediate consequences thereof. Transition-state environment can be altered by the addition of massive amounts of salt. The salt, however, must not interfere in the reaction by capturing any intermediates that might be formed; neither should it have significant nucleophilic character toward epoxide substrates; nor should the cation selectively complex with the substrate. Sodium perchlorate was selected because it seemed to meet all of these requirements, and thus its effect upon the products of epoxide ring opening was examined.

Experimental Section

Chemicals. Tetramethylethylene oxide (TMEO) was synthesized and

---

(1) Support of this work by grants from the National Institutes of Health of the U.S. Public Health Service and the National Science Foundation is gratefully acknowledged. Part 4 of the continuing study devoted to the examination of the role of epoxides in vicinal diol dehydration. Part 3: Y Pocker and B. P. Ronald, *J. Am. Chem. Soc.*, **100**, 3122-3127 (1978).

(2) Visiting Scholar in the Department of Chemistry, University of Washington, during the period 1978-1979 while on sabbatical leave from the Department of Chemistry, Idaho State University, Pocatello, Idaho.

(3) (a) F. A. Long and W. F. McDevit, *Chem. Rev.*, **51**, 119 (1952); W. F. McDevit and F. A. Long, *J. Am. Chem. Soc.*, **74**, 1773 (1952); (b) C. K. Ingold, "Structure and Mechanism in Organic Chemistry", 2nd ed., Cornell University Press, Ithaca, N.Y., 1969, Chapters 7 and 9.

(4) S. Winstein and E. Clippinger, *J. Am. Chem. Soc.*, **78**, 2784-2788 (1956); S. Winstein, P. E. Klinedinst, Jr., and G. C. Robinson, *ibid.*, **83**, 885-595 (1961); S. Winstein and B. Appel, *ibid.*, **86**, 2718-2720, 2720-2721 (1964).

(5) (a) I. M. Kolthoff, *Experientia, Suppl. V*, **33** (1956), and references cited therein; (b) E. Grunwald, S. Highsmith, and Ting-Po I in "Ions and Ion-Paris in Organic Reactions", Vol. II, M. Szwarc, Ed., Wiley, New York, 1974.

(6) S. Winstein, B. Appel, R. Baker, and A. Diaz, *Chem. Soc., Spec. Publ.*, No. **19**, 109 (1965), and references cited therein.

(7) Y. Pocker and R. F. Buchholz, *J. Am. Chem. Soc.*, **92**, 2075-2084, 4033-4038 (1970); **93**, 2905-2909 (1971); Y. Pocker and D. L. Ellsworth, *ibid*, **99**, 2276-2284, 2284-2293 (1977).

(8) R. A Robinson and R. H. Stokes, "Electrolyte Solutions", 2nd revised ed., Bulterworths, London, 1959, Chapter 14.

(9) Y. Pocker and B. P. Ronald, *J. Am. Chem. Soc.*, **100**, 3122-3127 (1978).

0002-7863/80/1502-5311$01.00/0